Catalysis Today 164 (2011) 186–189

Contents lists available at ScienceDirect

Catalysis Today

journal homepage: www.elsevier.com/locate/cattod

Enhancement of electrochemical stability and catalytic activity of Pt nanoparticles via strong metal-support interaction with sulfur-containing ordered mesoporous carbon

Kyungjung Kwon[a,b], Seon-ah Jin[a], Chanho Pak[a,*], Hyuk Chang[a], Sang Hoon Joo[a,c], Hyung Ik Lee[d], Jin Hoe Kim[d], Ji Man Kim[d,**]

[a] Energy Lab, Emerging Tech. Research Center, Samsung Advanced Institute of Technology, Samsung Electronics, San #14-1, Nongseo-dong, Giheung-gu, Yongin, Gyeonggi-do 446-712, Republic of Korea
[b] Department of Energy & Mineral Resources Engineering, Sejong University, Seoul 143-747, Republic of Korea
[c] School of Nano-Bioscience & Chemical Engineering (NBC) and Interdisciplinary School of Green Energy, Ulsan National Institute of Science and Technology (UNIST), BanYeon-Ri 100, Ulsan 689-805, Republic of Korea
[d] Department of Chemistry, BK21 School of Chemical Materials Science and Department of Energy Science, Sungkyunkwan University, Suwon, Gyeonggi-do 440-746, Republic of Korea

ARTICLE INFO

Article history:
Available online 3 November 2010

Keywords:
Pt nanoparticle
Sulfur
Stability
Oxygen reduction
Strong metal-support interaction
Ordered mesoporous carbon

ABSTRACT

Pt nanoparticles on sulfur-containing ordered mesoporous carbon (Pt/S-OMC) are obtained with 3 nm in size and 60 wt.% loading. XPS analysis shows that there is a strong metal-support interaction between Pt nanoparticles and S atoms embedded on the OMC support. This strong metal-support interaction fastens Pt nanoparticles upon the support and alters the electronic state of Pt from Pt^0 of bulk Pt to a slightly charged state of $Pt^{\delta+}$. These features result in an improvement both in electrochemical stability and oxygen reduction reaction kinetics compared to Pt/OMC where the OMC does not have sulfur atoms. The approach of tuning the electronic state and the interaction of Pt on carbon supports by embedding heterogeneous atoms into the OMC can effectively improve the stability and catalytic activity of Pt nanoparticles.

1. Introduction

To develop highly active catalysts for the fuel cell application, new types of nano-structured carbon materials have been actively pursued. Among the nano-structured carbon materials, the use of ordered mesoporous carbon (OMC) as the catalyst support has attracted an increasing attention in recent years [1]. The OMC exhibits intriguing structural properties that are favorable for the fuel cell application, including large surface area, highly interconnected mesopores and graphitic framework microstructures for the pathways of electrons.

The catalyst stability is a very important property to ensure the durable operation of fuel cell system. Thus, there have been various attempts with the modification of surface properties of carbon supports to increase the interaction between metal nanoparticles and the supports [2–5]. Among them, the addition of heterogeneous atoms such as nitrogen and sulfur to carbon supports has been reported to be beneficial to the stability of Pt catalysts [3–5]. Generally, sulfur-containing impurities in fuel or air are Pt-poisoning species because of the strongly adsorbing nature of sulfur onto Pt surface [6]. However, the strong interaction between platinum and sulfur can be utilized for the design of a stable Pt–S–C catalyst system. Contrary to the previous approaches where sulfur-containing functional groups are adsorbed onto carbon and sulfur atoms remains on the carbon surface as a result of heat treatment [5,7,8], sulfur atoms can be directly incorporated into carbon framework in the preparation process of OMC. The authors recently reported that the thermal stability of Pt nanoparticles was improved significantly by using the strong metal-support interaction between Pt metal atoms and sulfur atoms in the sulfur-containing OMC (S-OMC) [9]. In this study, the effect of sulfur addition to Pt/OMC system on the electrochemical stability and catalytic activity for oxygen reduction reaction in the acidic condition is investigated.

2. Materials and methods

The OMC supports were synthesized via a nano-replication method using the calcined ordered mesoporous silica (OMS) template. For the synthesis of S-OMC, a solution containing *p*-toluenesulfonic acid (TSA) and acetone was infiltrated into the calcined OMS template. The S-OMC supports can be obtained by

* Corresponding author. Tel.: +82 31 280 6884; fax: +82 31 280 9359.
** Corresponding author. Tel.: +82 31 299 4177; fax: +82 31 299 4179.
E-mail addresses: chanho.pak@samsung.com (C. Pak), jimankim@skku.edu (J.M. Kim).

0920-5861/$ – see front matter © 2010 Elsevier B.V. All rights reserved.
doi:10.1016/j.cattod.2010.10.030

Table 1
Physicochemical properties of OMC, S-OMC, Pt/OMC and Pt/S-OMC.

	S_{BET}[a] (m^2/g)	D_{BJH}[b] (nm)	S content (wt.%)	Initial Pt particle size[c] (nm)
OMC	1414	4.4	0	–
S-OMC	1030	5.0	2.3	–
Pt/OMC	–	–	–	3.76
Pt/S-OMC	–	–	–	3.14

[a] BET surface areas calculated in the range of p/p_0 = 0.05–0.20.
[b] BJH pore sizes obtained from the adsorption branches.
[c] Pt particle size estimated by Scherer equation from (1 1 1) peaks in the XRD patterns.

a series of heat treatment and removal of the OMS template. The OMC supports without sulfur were prepared by the same method as S-OMC except for utilizing a solution containing furfuryl alcohol, sulfuric acid and ethanol instead of the TSA solution. Pt/OMC and Pt/S-OMC were prepared by incipient wetness method resulting in the virtually same Pt particle size and loading (the particle size of ca. 3 nm and the Pt loading of 60 wt.%). Details on the preparation and physical properties of OMC, S-OMC, Pt/OMC and Pt/S-OMC can be found in our previous report [9] and some selected properties are summarized in Table 1.

Structural and compositional analyses such as transmission electron microscopy (TEM) and X-ray photoelectron spectroscopy (XPS) were conducted similarly to the previous report [9]. The electrochemical stability and catalytic activity of Pt/OMC, Pt/S-OMC were evaluated with a rotating disk electrode (RDE) apparatus (Princeton Applied Research) at room temperature. The preparation of thin-film working electrode and the half-cell configuration were as mentioned in the previous report [9]. Cyclic voltammetry (CV) for evaluating the electrochemical surface area (ECSA) of the catalyst was conducted at a scan rate of 50 mV/s in the potential window from 0.05 V to 1.2 V vs. reversible hydrogen electrode (RHE) with nitrogen-saturated 0.1 M $HClO_4$ electrolyte. The change in oxygen reduction catalytic activity during a potential cycling test was measured at a scan rate of 10 mV/s and a rotation speed of 900 rpm with oxygen-saturated 0.1 M $HClO_4$ electrolyte [10,11].

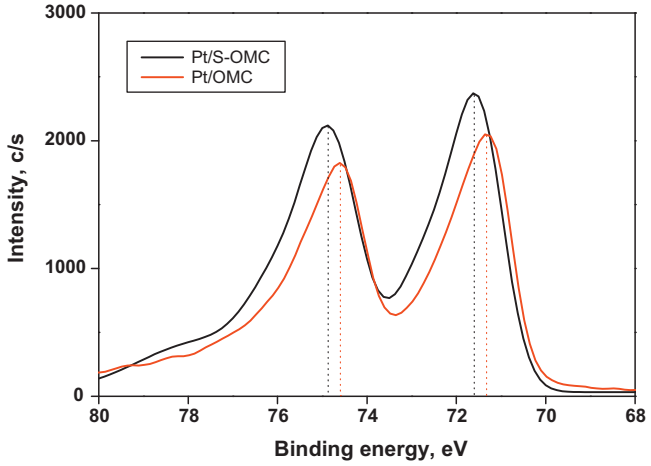

Fig. 1. XPS spectra of Pt 4f in Pt/S-OMC and Pt/OMC.

3. Results and discussion

As reported in our previous study [9], the electronic state of Pt nanoparticles on S-OMC is different from that on the OMC. Fig. 1

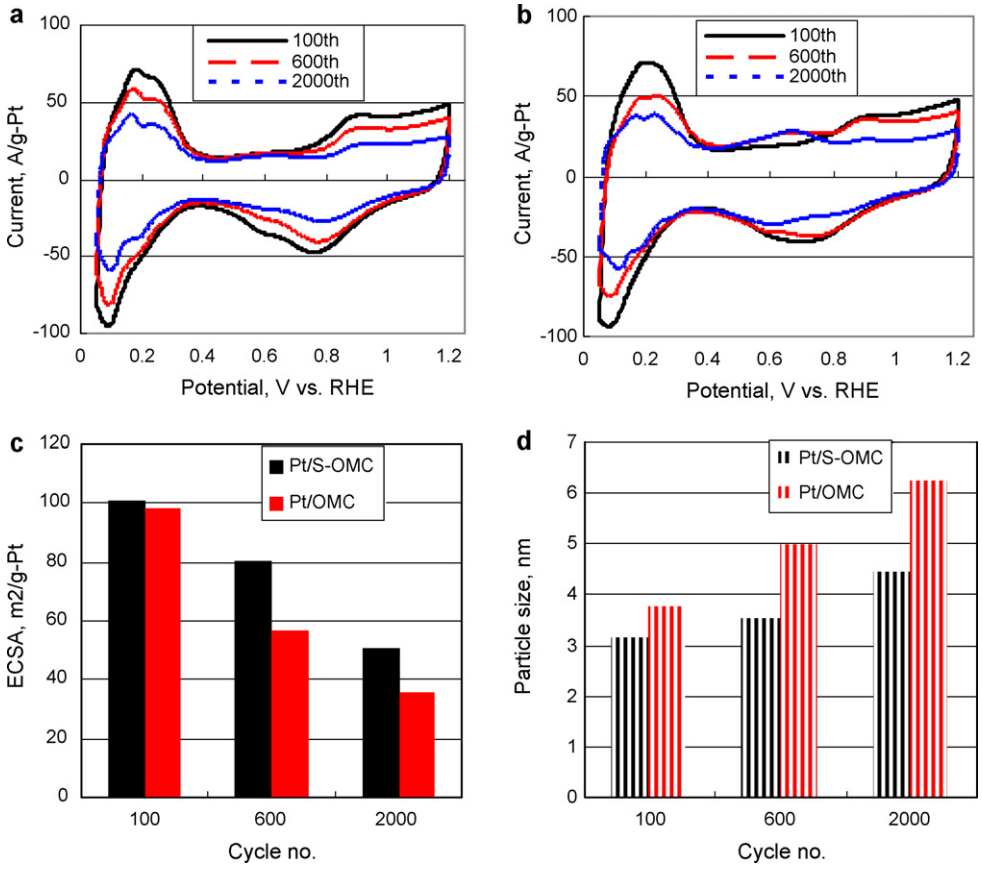

Fig. 2. Cyclic voltammetry of (a) Pt/S-OMC and (b) Pt/OMC for 2000 cycles. (c) ECSA and (d) estimated particle size of Pt/S-OMC and Pt/OMC during the cyclic voltammetry.

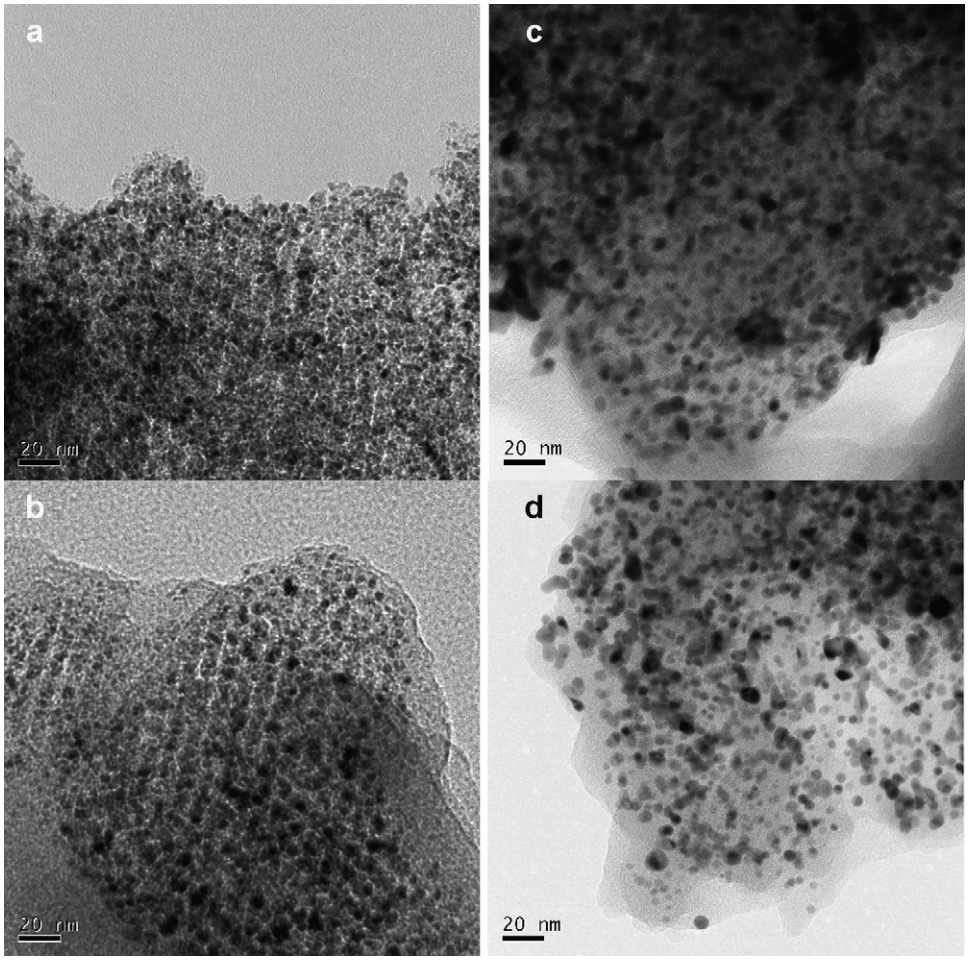

Fig. 3. TEM images of (a) Pt/S-OMC after the 100th cycle, (b) Pt/OMC after the 100th cycle, (c) Pt/S-OMC after the 2000th cycle, and (d) Pt/OMC after the 2000th cycle.

shows the Pt 4f XPS spectra of Pt/S-OMC and Pt/OMC. The binding energy of Pt/S-OMC shifts to a higher value compared to Pt/OMC by an increment of 0.3 eV. The increased binding energy is less than that of oxidized Pt species and corresponds to a slightly charged state (δ^+) of Pt nanoparticles originating from the charge transfer from Pt nanoparticles to S atoms. The positive shift in binding energy of Pt in contact with sulfur was also observed for the Pt atoms on thiolated carbon nanotubes [8] and a similar level of binding energy shift of Pt nanoparticles was reported for the surface modification of Pt nanoparticles with organic ligands [12].

The electrochemical stability of Pt/S-OMC was determined in an accelerated stability test by continuously applying linear potential sweeps from 0.05 V to 1.2 V, which causes surface oxidation/reduction cycles of Pt nanoparticles. Fig. 2(a) and (b) are the cyclic voltammograms of Pt/S-OMC and Pt/OMC for 2000 cycles, repectively. The ECSA in Fig. 2(c) was calculated from the amount of electrical charge in the hydrogen desorption peak with the consideration of the double layer charging current. Because of the existence of some adsorbed impurities on the catalyst surface and the gradual wetting of Nafion® film on the catalyst, the actual decrease in ECSA is not observed in the initial tens of cycles [11]. The cyclic voltammetry of Pt/S-OMC and Pt/OMC in the first 100th cycle shows the typical electrochemical behavior of Pt nanoparticles. However, a redox peak around 0.6 V starts to develop during the cycling test in the case of Pt/OMC. Whereas Pt/S-OMC maintains its general shape of cyclic voltammogram throughout the cycling test, Pt/OMC has some changes in cyclic voltammogram including the evolution of the redox peak, which implies the surface reconfiguration of the catalyst during the cycling test.

The initial ECSA of the catalysts is about 100 m^2/g-Pt (surface area normalized by Pt content), which is a reasonable value with the consideration of initially similar Pt particle sizes of Pt/S-OMC (3.14 nm) and Pt/OMC (3.76 nm). Because the particle size estimation from the ex situ TEM analysis of RDE catalyst sample could be misleading particularly for nanoparticles inside carbon mesopores, the Pt particle size was estimated in Fig. 2(d) on the assumption of uniform particle growth of the catalysts based on the initial particle size determined by X-ray diffraction method. Although the general trend of decreasing ECSA and increasing particle size during the cycling test applies to both kinds of catalysts, the ECSA reduction rate and the corresponding particle growth rate is faster for Pt/OMC. Considering the mesopore size of S-OMC (5.0 nm) and OMC (4.4 nm), the growth of Pt nanoparticles inside the mesopore results in a contact with mesopore walls and, eventually, a penetration through the carbon framework. The average Pt particle size on the OMC is larger than the pore size of OMC from the 600th cycle and the expected collapse of OMC pore structure is reflected in the cyclic voltammetry of Pt/OMC (Fig. 2(b)). As mentioned, the redox peak around 0.6 V can be attributed to the catalyst structure reconfiguration where a newly exposed surface functional group (presumably quinine–hydroquinone) on the collapsed OMC walls acts as a redox couple [13]. The average Pt particle size on the S-OMC at the end of the cycling test is less than the corresponding particle size of Pt/OMC and the mean pore size of S-OMC, which indicates that Pt supported on the S-OMC is more stable than Pt supported on the OMC.

The TEM images of the catalysts after the 100th and the 2000th cycle are compared in Fig. 3. For the first 100th cycle, the catalysts

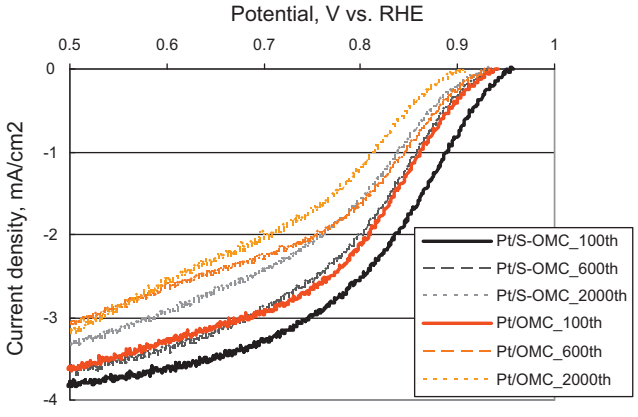

Fig. 4. Polarization curves for the oxygen reduction reaction on Pt/S-OMC and Pt/OMC after the 100th cycle, 600th cycle and 2000th cycle.

maintain a regularly developed mesopore structure and a good particle dispersion with an average size around 3.5 nm. The growth and aggregation of Pt nanoparticles are clearly seen in the TEM images after the 2000th cycle. The mesopore structure of Pt/OMC appears to collapse completely with a mostly amorphous feature as we expect from the larger Pt particle size after the 2000th cycle than the mesopore size of OMC. The mesopore structure of Pt/S-OMC after the cycling test is barely observable such as the slightly crystalline characteristic of the carbon support in the small region of less Pt particle population. It was difficult to obtain a conclusive TEM image for the well-maintained pore structure of Pt/S-OMC after the 2000th cycle although the average Pt particle size on the S-OMC is slightly less than the mean mesopore size of S-OMC. Because it is inevitable that the Pt particle size has some ranges of distribution, large particles over the mean particle size would start to grow against the mesopore walls earlier in the cycling test than we expect from the analysis based on the mean particle and mesopore sizes.

Cyclic voltammetry was interrupted after the 100th cycle, 600th cycle and 2000th cycle and polarization curves for the oxygen reduction catalytic activity on Pt/S-OMC and Pt/OMC are shown in Fig. 4. The initial oxygen reduction catalytic activity of Pt/S-OMC is superior to that of Pt/OMC as reported for the enhanced catalytic activity of Pt on thiolated carbon nanotubes [7]. Considering the similar Pt particle size on the S-OMC and the OMC, the improved oxygen reduction kinetics might result not from the size effect but from the change in electronic state of Pt nanoparticle. The higher catalytic activity of Pt/S-OMC than Pt/OMC at the same cycle number is maintained until the end of the cycling test and this can be attributed to the smaller particle size of Pt/S-OMC [10].

4. Conclusions

Pt/S-OMC shows a strong metal-support interaction between Pt nanoparticles on the support and S atoms embedded on the OMC support as confirmed by the Pt 4f XPS result. This interaction results in an improvement both in electrochemical stability and oxygen reduction catalytic activity compared to Pt/OMC. The incorporation of sulfur into the OMC support suppresses the growth of Pt nanoparticles so that the advantage of using OMC as a support material, which has a large surface area and a facile mass transfer of oxygen, can be further taken. In addition, the approach of incorporating S atoms into the OMC framework to modify the electronic state of Pt nanoparticles can be widened for other kinds of heterogeneous atoms in the OMC.

Acknowledgements

J.M. Kim thanks to the WCU (World Class University) program through the National Research Foundation (NRF) of the Korea funded by the Ministry of Education, Science and Technology (R31-2008-000-10029-0) and the Basic Science Research program (NRF, 2009-0076903) for financial support.

References

[1] H. Chang, S.H. Joo, C. Pak, J. Mater. Chem. 17 (2007) 3078–3088.
[2] R. Kou, Y. Shao, D. Wang, M.H. Engelhard, J.H. Kwak, J. Wang, V.V. Viswanathan, C. Wang, Y. Lin, Y. Wang, I.A. Aksay, J. Liu, Electrochem. Commun. 11 (2009) 954–957.
[3] Y. Zhou, R. Pasquarelli, T. Holme, J. Berry, D. Ginley, R. O'Hayre, J. Mater. Chem. 19 (2009) 7830–7838.
[4] Y. Chen, J. Wang, H. Liu, R. Li, X. Sun, S. Ye, S. Knights, Electrochem. Commun. 11 (2009) 2071–2076.
[5] S.C. Roy, P.A. Christensen, A. Hamnett, K.M. Thomas, V. Trapp, J. Electrochem. Soc. 143 (1996) 3073–3079.
[6] R. Mohtadi, W.-K. Lee, J.W. Van Zee, J. Power Sources 138 (2004) 216–225.
[7] Y.-T. Kim, T. Mitani, J. Catal. 238 (2006) 394–401.
[8] Y.-T. Kim, T. Uruga, T. Mitani, Adv. Mater. 18 (2006) 2634–2638.
[9] H.I. Lee, S.H. Joo, J.H. Kim, D.J. You, J.M. Kim, J.-N. Park, H. Chang, C. Pak, J. Mater. Chem. 19 (2009) 5934–5939.
[10] J. Zhang, K. Sasaki, E. Sutter, R.R. Adzic, Science 315 (2007) 220–222.
[11] B. Merzougui, S. Swathirajan, J. Electrochem. Soc. 153 (2006) A2220–A2226.
[12] X.Y. Fu, Y. Wang, N.Z. Wu, L.L. Gui, Y.Q. Tang, J. Colloid Interface Sci. 243 (2001) 326–330.
[13] N.P. Subramanian, S.P. Kumaraguru, H. Colon-Mercado, H. Kim, B.N. Popov, T. Black, D.A. Chen, J. Power Sources 157 (2006) 56–63.